COMMUNICATIONS
FROM THE
KONKOLY OBSERVATORY
OF THE
HUNGARIAN ACADEMY OF SCIENCES

MITTEILUNGEN
DER
STERNWARTE
DER UNGARISCHEN AKADEMIE
DER WISSENSCHAFTEN

BUDAPEST — SZABADSÁGHEGY

No. 82.

M. PAPARÓ and L. G. BALÁZS

DISTRIBUTION OF STARS OF SPECTRAL TYPES EARLIER THAN F7 AROUND IC 4665

BUDAPEST, 1982

ISBN 963 8361 17 4
HU ISSN 0324 - 2234
Felelős kiadó: Szeidl Béla

Hozott anyagról sokszorosítva

8213659 MTA KESZ Sokszorosító, Budapest. F. v.: dr. Héczey Lászlóné

DISTRIBUTION OF STARS OF SPECTRAL TYPES EARLIER THAN F7 AROUND IC 4665

ABSTRACT

A study was made of the spatial distribution of early type stars in a region of intermediate galactic latitude. Objective prism plates were used to survey an area of 19.5 $\square^{\circ}$ around the cluster IC 4665 for all stars of spectral types earlier than F7 down to $12^{m}.5$ photographic magnitude. 427 stars were detected, for which spectral types and photographic UBV colours were obtained. Different amounts of interstellar reddening were derived for the $l<30^{\circ}$ and $l>30^{\circ}$ parts of the region. Separate absorption correction was made for each of the parts. The stars were divided into four groups: spectral type A1 and earlier, A2 - A7, A8 - F2 and F3 - F7, and the space densities were determined for each group. The shape of the space density curve of the A2 - A7 stars reveals the existence of two kinematic subgroups. The velocity dispersions characterizing these two subsystems have a ratio of 1:1.6. The interpretation of space density curves of stars earlier than A2 in terms of such subgroups faces difficulties because of the possible photometric distance scale error and the interference with the Gould belt.

INTRODUCTION

The logarithmic density of A type stars plotted against distance from the galactic plane displays an inflexion point. It is difficult to reconcile this point with a pure Gaussian velocity distribution assuming the stars to be distributed in plane parallel layers (*Woolley*, 1965). *Oort* (1932) wrote in his classical paper " that the velocity distribution is usually found to deviate somewhat from Gaussian distribution. However it can always be represented by a sum of two or three Gaussian components with different moduli. " Later *Van Rhijn* (1960) suggested that the dispersion in the linear velocity of A type stars increases with distance from the galactic plane. He claimed that two groups of A type stars with different dispersions can be found. Space density curves displaying these characteristics have been published, for instance, by *Kurochkin* (1958), *Upgren* (1962,1963), *Woolley* and *Steward* (1967), *Borzov* (1973) and *Balázs* (1975, hereafter referred to as Paper I). *Balázs* found that plotting the density ratios at z=0 of the two subsystems versus spectral type a jump can be seen on the curve at spectral type A0. He interpreted this

characteristic as a consequence of the discontinuous generation of stars and derived the time difference between the two birth events by the lifetime of stars at which the jump appeared on the curve. The possible cosmogonical significance of this jump on the curve needs further investigations using homogeneous stellar samples observed in different galactic directions to avoid misinterpretations of incomplete and inhomogeneous data.

The aim of the present work is to continue the investigation to get an overall picture about the spatial density distribution of stars with different spectral types around the Sun at intermediate galactic latitudes.

OBSERVATIONAL MATERIAL

An area of 19.5$\square^{\circ}$ centred on $l^{II}=30^{\circ}.74$, $b^{II}=15^{\circ}.98$ ($\alpha=17^{h}48^{m}$, $\delta=5^{\circ}20'$) was investigated. The observations were carried out with the 60/90/180 cm Schmidt telescope of the mountain station of Konkoly Observatory. Spectral types and UBV colours were obtained for 427 stars brighter than $12^{m}.5$ photographic magnitude. The spectral types are based on three objective prism plates taken with a 5° UBK 7 (UV transmitting) prism that gives a dispersion of 580 Å/mm at H_{γ}. Kodak IIa-O emulsions were used and the widening was 18'', equivalent to 0.16 mm on the plate. The plates were made with double exposures of 6^{m} and 24^{m}, so that any systematic variations in the classification with photographic density could be estimated.

The UBV photometry is based on five plates in B and in U and on four plates in V. The emulsion types, filters and exposure times used are given in the following table:

	emulsion	filter	exp. time
U	Kodak 103a-O	Schott UG1 2mm	10^{m}
B	Kodak 103a-O	Schott GG13 2mm	5^{m}
V	Kodak 103a-D	Schott GG14 2mm	4^{m}

The relationships between the international system and the instrumental system are given by the following equations:

$$V_{instr} = V - 0.16(B-V) + 0.10$$

$$(B-V)_{instr} = 1.05(B-V) - 0.02$$

$$(U-B)_{instr} = 1.01(U-B) + 0.11(B-V) - 0.03$$

The plates were measured with Konkoly Observatory's Cuffey type iris photometer. The photoelectric sequence given by *Alcaino* (1965) was partly used and the four faintest stars were obtained with Konkoly Observatory's 50 cm Cassegrain telescope. The mean errors of the photographically determined colours are ±0.07 ±0.06 and ±0.05 for U,B and V, respectively.

The spectral classification was based on the criteria given by *Stock* and *Slettebak* (1959), *Stock* (1971) and *Seitter* (1975). The classification using small scale spectra, however, is somewhat uncertain with late B and early A type stars because the hydrogen lines dominating the spectra of these stars reach their maximum strength and show little change with spectral type. Therefore an independent method, the Q method of *Becker* (1963) was used to determine the spectral types of stars earlier than A0.

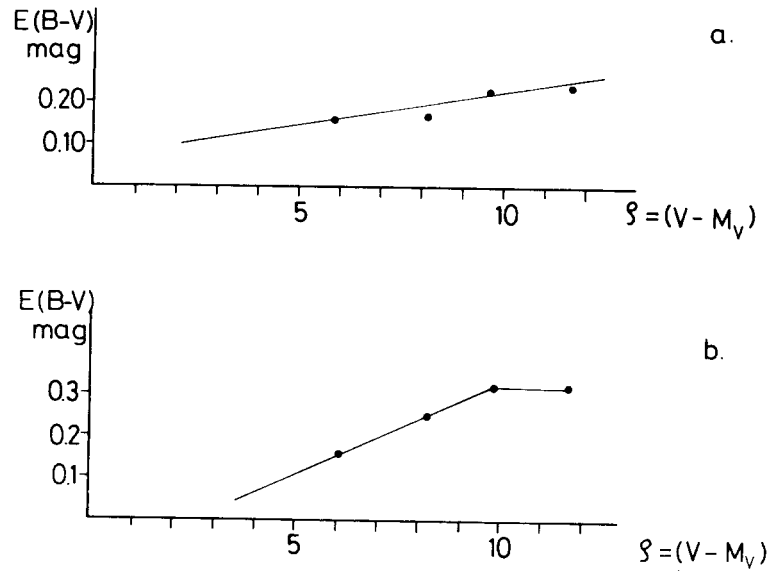

Fig. 1a-b The colour excesses (E_{B-V}) as functions of uncorrected distance moduli. (a: $l>30^{\circ}$, b: $l<30^{\circ}$)

After getting the colours of stars, Q = (U-B)- 0.72(B-V) values were calculated and spectral types were estimated. The differences between the spectral classes obtained by the two different methods were, except for a few cases, less than two subclasses. Finally the arithmetic mean of these two spectral classes was used.

INTERSTELLAR REDDENING

Adopting *Allen*'s (1973) relation between intrinsic colour index and spectral type, the E_{B-V} and E_{U-B} colour excesses were obtained. *Allen*'s relation between absolute magnitude and spectral type was used to compute the distance modulus for each star. The stars were divided into four groups according to their distance modulus: $<7^m$, 7^m-9^m, 9^m-11^m and $>11^m$. The mean distance modulus and the colour excesses were determined for each subgroup. The distribution of interstellar matter is inhomogeneous in this field. *FitzGerald* (1968) has shown that the $l^{II}<30^o$, $b=15^o$ and $l^{II}>30^o$, $b=15^o$ fields have different amounts of absorption. Up to 1500 pc for the former field he obtained $0.3\leq E_y<0.6$, for the latter one till 1000 pc the value $0.1\leq E_y<0.2$ is given. Adopting this result a line at $l^{II}=30^o$, parallel to the galactic axis was drawn on the plate and the absorption was determined separately on both sides of this line. The colour excesses determined by this method are plotted in Fig. 1/b for the $l^{II}<30^o$ side and Fig. 1/a for the $l^{II}>30^o$ side of the line, as a function of the distance modulus. It can be seen from this figure that a more dense absorbing material is situated on the $l^{II}<30^o$ side of the plate. The cluster IC 4665 has a distance modulus of $7^m.8$ according to *Alcaino* (1965). The $E_{B-V} = 0^m.17$ value at a distance modulus of $7^m.8$ obtained from Fig. 1/a is in good agreement with $E_{B-V} = 0^m.152$ given by *Alcaino* and with $E_{B-V} = 0^m.17$ given by *Hogg* and *Kron* (1955). Adopting E_{B-V} from Fig. 1/a and 1/b and a ratio of total to selective absorption equal to 3.0, the magnitudes were corrected for the absorption.

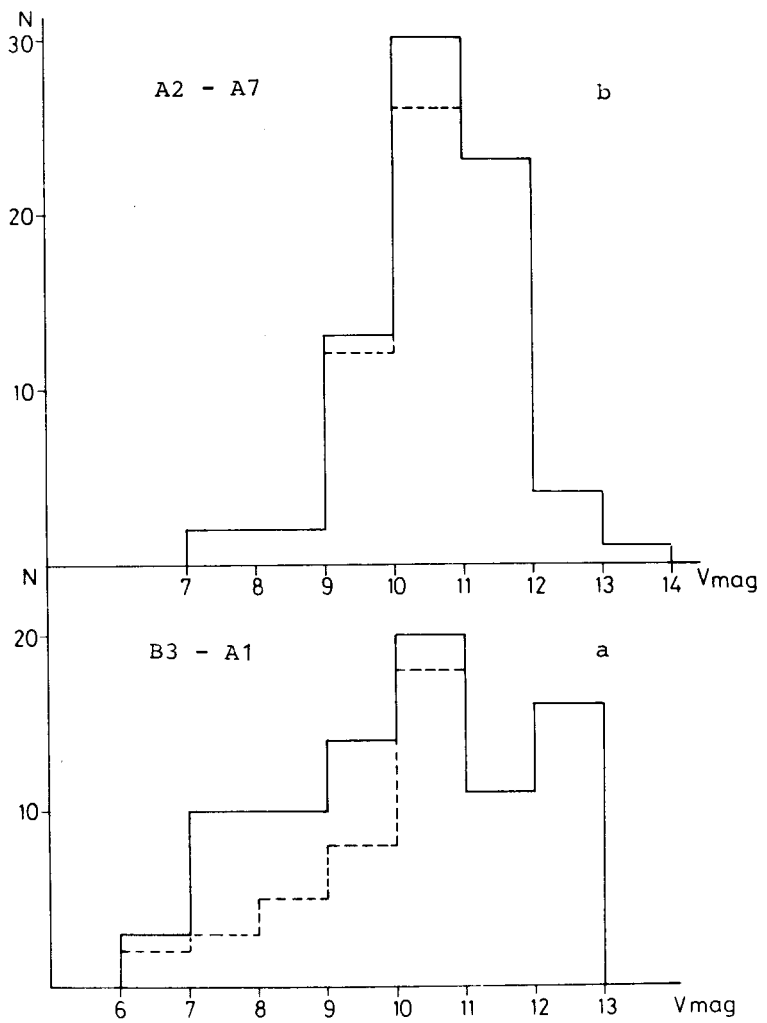

Fig. 2a-b The distributions of stars against the V magnitudes. Dashed lines indicate the corresponding distributions after excluding the cluster members of IC 4665.

The limiting magnitude of our plates is generally $12^{m}.5$. Based on the sharpness of classificational criteria and on the number of stars in each subclass four subgroups were separated: stars earlier than A2, A2 - A7, A8 - F2 and F3 - F7. The distribution of stars against the V measured magnitude in the given subgroups is shown in Fig. 2a-d. Dashed lines indicate the cor-

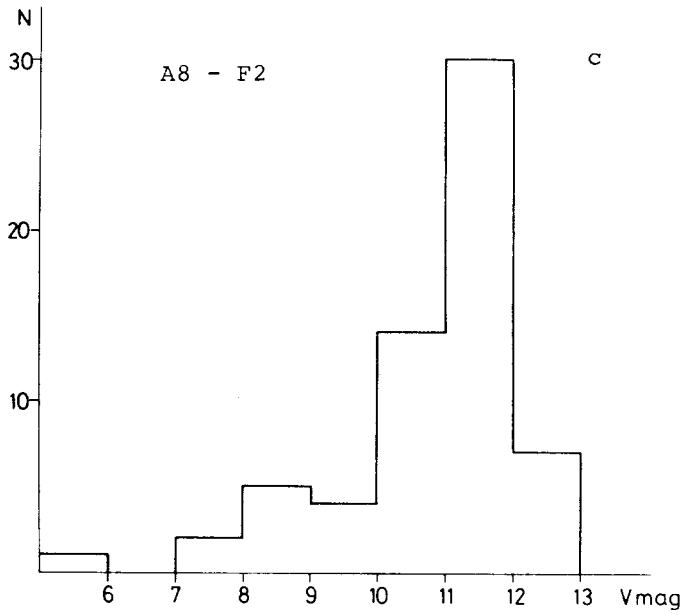

Fig. 2c The distribution of stars against the V magnitude.

responding distributions after excluding the cluster members of IC 4665 defined by *Alcaino* (1965). After correcting the magnitudes for interstellar absorption the basic convolution equation of stellar statistics

$$A(m) = \int_{-\infty}^{+\infty} D(y)\,\Phi(m-y)\,dy$$

can be solved separately for each subgroup. As usual, A(m) is the

number of stars in the apparent magnitude interval $(m-\delta m, m+\delta m)$; $D(y)$ is the number of stars between distance moduli $(y-\delta y, y+\delta y)$; and $\Phi(m-y)$ is the luminosity function of a given spectral and

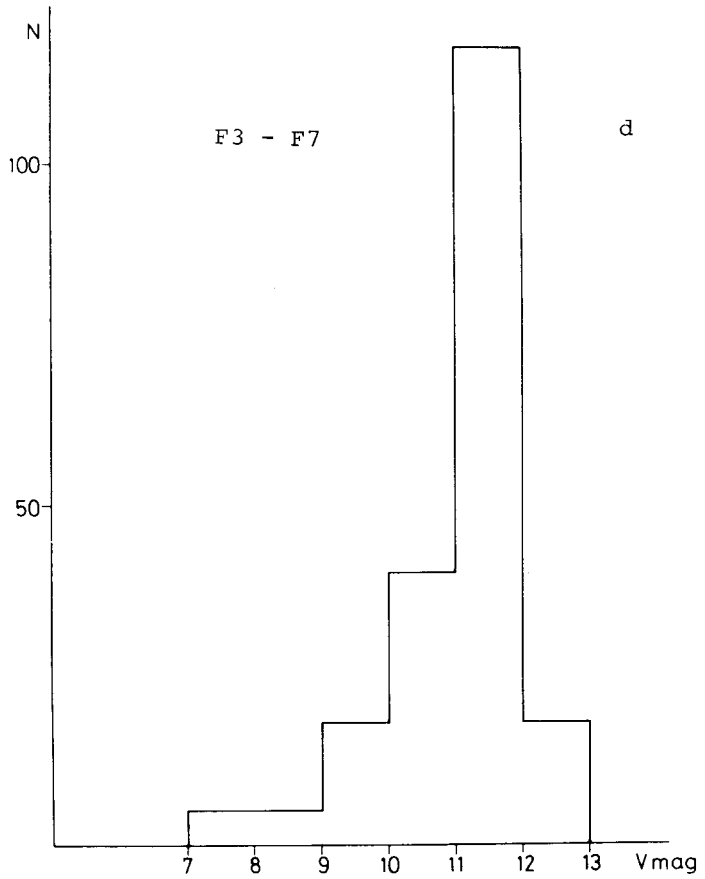

Fig. 2d The distribution of stars against the V magnitude.

luminosity class. Following *McCuskey* (1966) the form of Φ is a Gaussian function. Its mean absolute magnitude and standard deviation were taken from *Allen* (1973). To solve the equation the matrix method described by *Dolan* (1974) was used. The densities derived by this method are plotted in Fig. 3a-d. The dashed lines show the plate limit. Bars indicate the 1σ error bars obtained by *Dolan*'s method.

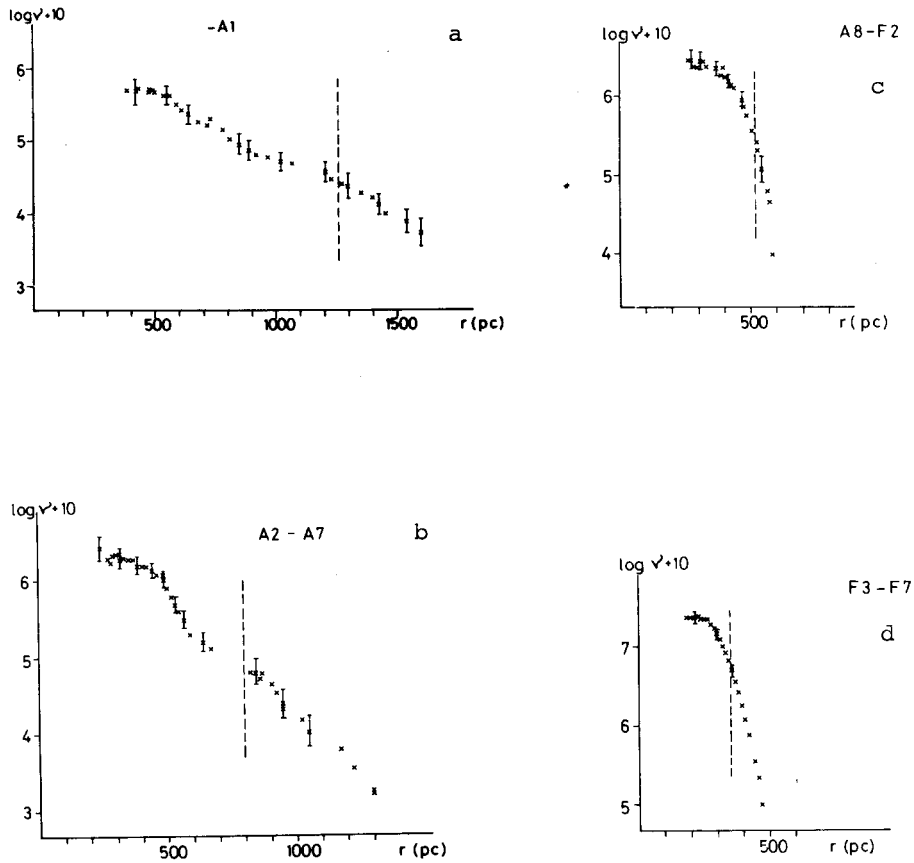

Fig. 3a-d The derived space densities of the different subgroups.
(The dashed lines show the plate limit.)

DISCUSSION OF THE SPACE DENSITIES

Except for the subgroup earlier than A2 the density gradients ($\partial\nu/\partial r$) are nearly the same up to 600 pc if the plate limit allows the determination of space densities up to this distance at all. At about 600 pc the density gradient of A2 - A7 stars changes and becomes smaller. The space density of stars earlier than A2 also displays similar characteristics, i.e. steeper gradient up to 900 pc and a change to a slower decrease afterwards. The gradient at the first part of the curve, however, is not so steep as in the case of A2 - A7 stars and it needs some further remarks. We shall return to this problem later.

As was pointed out previously (Paper I) the spatial distribution of the A stars near to the galactic poles shows a similar form to stars in some intermediate latitude galactic fields if the densities in line of sight were plotted against the corresponding z distances perpendicular to the galactic plane. The similarity between these distributions and those obtained by the present investigation therefore suggests that the density gradients are mainly due to the contributions of the gradients perpendicular to the galactic plane to the gradients in the line of sight. This result enables us to compute a relation connecting the spatial density, the standard deviation of the z velocity component and the gravitational potential, following the procedure outlined in Paper I. As a result we could get a curve for $(\sigma_z(z),z)$ plane characterizing the z dependence of σ_z.In the case of a Gaussian distribution of z velocities we should get a horizontal line in this diagram because in that case $\sigma_z(z)$ is independent of z. However, after computing the $\sigma_z(z)$ curve according to the procedure of Paper I we obtained the curve displayed in Fig. 4 for A2 - A7 stars. The curve can be characterized by a slowly decreasing part up to 140 pc in z and a nearly horizontal part from 170 pc in z. The two parts are connected by a steep increase. This form of the $\sigma_z(z)$ curve might possibly indicate the coexistence of two kinematically distinct subsystems with different characteristic velocity dispersions. The smaller dispersion component deviates somewhat from Gaussian distribution because the $\sigma_z(z)$ curve is not quite horizontal. The larger dispersion component, however, is fairly Gaussian because of the

nearly horizontal run of $\sigma_z(z)$ in that part of the diagram. The density and $\sigma_z(z)$ are dominated by the small dispersion component at z<140 pc because the small dispersion component has a 5.4 times higher density in the plane of the Galaxy. At z>170 pc, however, the larger dispersion subsystem dominates the curves because of its slower density decrease. $\sigma_z(0)$ = 7.0 km/sec has been found in these computations. This value is close to that found in Paper I for a Lyra field. The run of $\sigma_z(z)$ at the small dispersion component deviates from pure Gaussian behavior. It might be interpreted by taking it into account that $\sigma_z(z)$ is based on the space density curve. Any systematic error in determining the space densities influences the shape of $\sigma_z(z)$. A very important source of systematic errors in determining the space densities by means of photometric parallaxes appears to be the lack of attention given to eliminate the effect of interstellar absorption from the photometric data. An overestimation of interstellar reddening causes a steeper and an underestimation a smaller density gradient than the true gradient in our case. As was

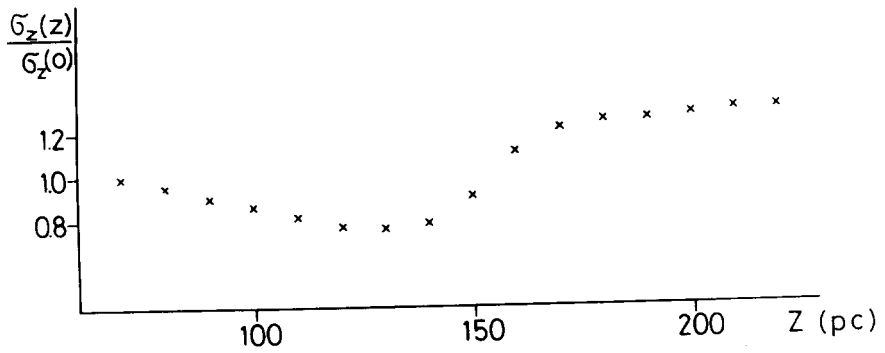

Fig. 4 The $\sigma_z(z)/\sigma_z(0)$ ratio computed from the density curve of A2 - A7 stars plotted against the hight (z) above the galactic plane.

mentioned earlier in this work the distribution of interstellar material is very patchy in this field and the western part contains more absorbing material than the eastern part. This was the

reason that the effect of interstellar absorption was evaluated for both parts separately. There was no way of determining the exact boundary between the lower and the higher absorbing region. We may expect, consequently, some over- or under-estimation in the absorption data. The absorbing material is concentrated at distance r<400 pc therefore that part of the space density curve could be distorted whereas at the remaining part only the distance scale is changed. The $0^m.24$ overestimation of the absorption corresponding to $0^m.08$ in E_{B-V} could account for the decreasing part of the $\sigma_z(z)$ curve. One could explain in this way the deflection of the $\sigma_z(z)$ curve from the pure Gaussian behaviour in the z<140 pc, region. The region z>140 pc, however, is little affected by absorption so it can be used to estimate the relative increase of σ_z between the two subsystems. The curve shows a 1:1.6 increase which is close to the value (1:1.8) was found in Paper I.

Let us now return to discuss the space density curve of stars younger than A2 in more detail. If one computed the $\sigma_z(z)$ plot in this case, following the procedure applied for A2 - A7 stars, one has $\sigma_z(0) = 10.2$ km/sec - a value which is a factor of 1.5 - 2 higher than was measured by direct kinematical methods for early type stars. Moreover the percentage of the larger dispersion component is somewhat higher (13%) contradicting what is expected for these stars. It is worth while to discuss two points which might have some significance.

1. The uncertainties in determining the absolute magnitudes of early type stars is somewhat higher than in stars having spectral types later than A2 because of the lack of good classificational criteria on our small scale spectra. The photometric Q method was applied to remove this uncertainty but a systematic error of one subclass could still remain. One subclass error corresponds to about $0^m.5$ at late B type stars and could satisfactorily explain a 1.26 times higher scale.
2. The possible scaling error could not explain the higher percentage of larger velocity dispersion stars among our early type stars in the galactic plane as was obtained in our calculations. The relative density of the two subsystems, namely, is invariant to the scale changes. The

interpretation of density curves in terms of velocity dispersions perpendicular to the galactic plane was based on the assumption that the observed density gradients were mainly due to the contributions of z gradient related in the line of sight. This assumption seemed not to work in this area. *Stothers* and *Frogel* (1974) pointed out that the system of B type stars within 1000 pc from the Sun is composed of two subsystems: stars concentrating to the galactic plane and stars concentrating to a plane bending about $18^{\circ} \pm 1^{\circ}$ to the plane of our system. These latter stars form the Gould belt. The Gould belt passes the northern part of our area surveyed and could therefore influence the space distribution of stars earlier than A2. The space distribution of stars later than A2, however, shows no signs of such influence because their density curve fits well to the curves observed in other galactic directions not affected by the Gould belt.

CONCLUSIONS

The uneven distribution of interstellar material in our field causes difficulties in eliminating the effect of interstellar absorption on photometric data. The shape of the space density curve of the A2 - A7 type stars reveals the existence of two kinematically distinct subsystems with different dispersions perpendicular to the galactic plane. The main characteristics of these subsystems are close to the values found in previous works in other galactic directions. The interpretation of space density curve of stars earlier than A2, in terms of the subsystems mentioned above, is not a simple matter because of the possible photometric distance scale error and the interference by the Gould belt.

ACKNOWLEDGEMENTS

The authors are indebted to Dr.M. Kun for valuable advice in space density computations. They are grateful to Mrs.I. Kálmán, Mr.I. Tóth and Mr.L. Sturman for their assistance in photometric measurements and analysing the data.

Budapest-Szabadsághegy, 15 October 1982

REFERENCES

Alcaino, G., 1965, Bull. Lowell Obs.No.7.167.

Allen, C.W., 1973, Astrophysical Quantities 3rd.ed., Athlona Press, London.

Balázs, L.G., 1975, Mitt.Sternwarte Ung.Ak.Wiss.No.68.(Paper I)

Becker, W., 1963, Application of Multicolor Photometry in " Basic Astronomical Data ",ed.K.Aa.Strand, Univ. Chicago Press, p.241.

Borzov, G.G., 1973, Astr.Zhu.50. 1041.

Dolan, J.F., 1974, Astron. and Astrophys.35. 105.

FitzGerald, M.P., 1968, Astron.J.73.983.

Hogg, A.R. and Kron, G.E., 1955, Astron.J.60.365.

Kurochkin, N.E., 1958, Astr.Zhu.35.86.

McCuskey, S.W., 1966, Vistas in Astronomy 7. 141.

Oort, J.H., 1932, B.A.N. 6. 249.

Seitter, W.C., 1975, Atlas for Objective Prism Spectra; Bonner Spectral Atlas II. Ferd. Dümmler Verlag, Bonn.

Slettebak, A. and Stock, J. 1959, Astr. Abhandlungen der Hamburger Sternwarte Bd.V.Nr.5.

Stock, J., 1971, Application of Objective Prism Techniques in the Magellanic Clouds in " The Magellanic Clouds ", ed.A.B. Muller, D.Reidel Publishing Co.,p.181.

Stothers, R. and Frogel, J.A., 1974, Astron.J.79.456.

Upgren, A.R., 1962, Astron.J.67. 37.

Upgren, A.R., 1963, Astron.J.68. 194.

Van Rhijn, P.J., 1960, Pub.Kapteyn Astr.Lab.Groningen No.61.

Woolley, R., 1965, Motions of the Nearby Stars in " Galactic Structure ", ed.A.Blaauw and M.Schmidt, Univ. Chicago Press, p.85.

Woolley, R. and Steward, J.M., 1967, MN.136.329.

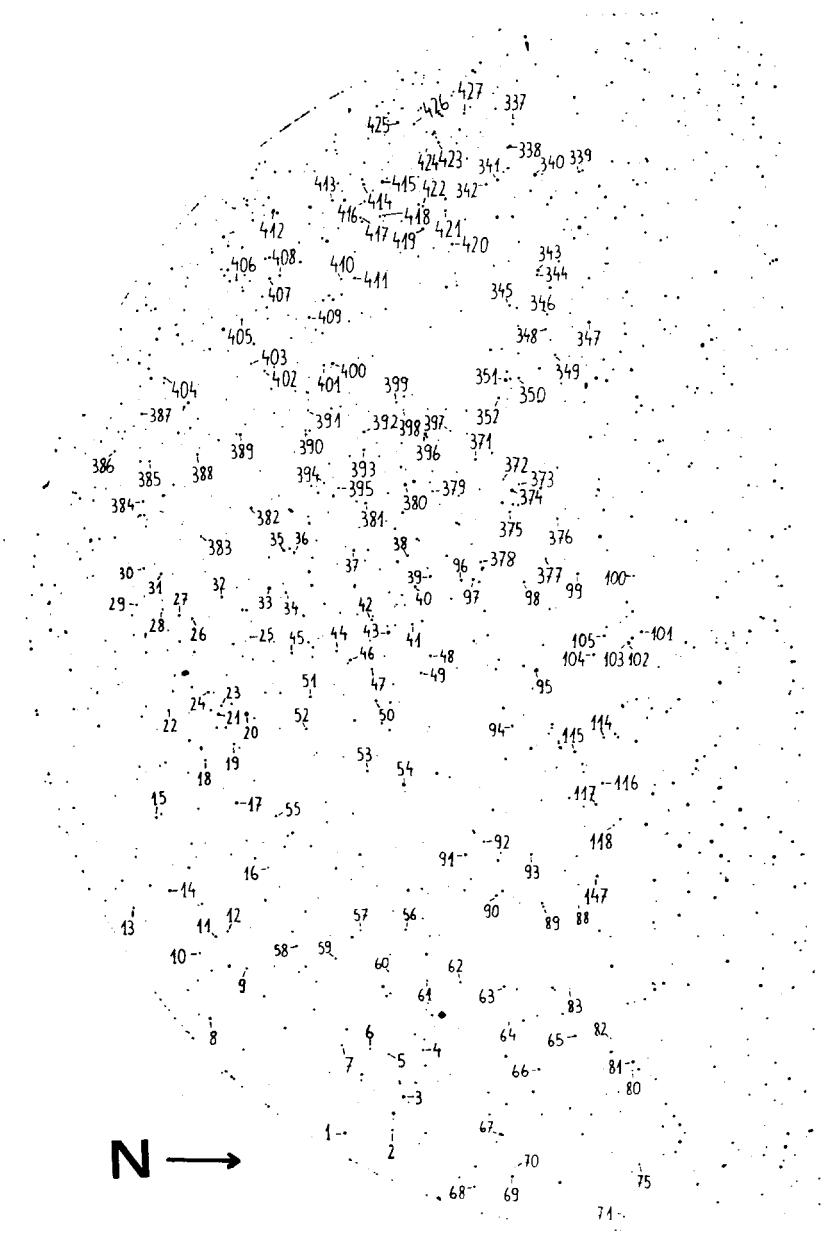

Finding chart of the survey stars

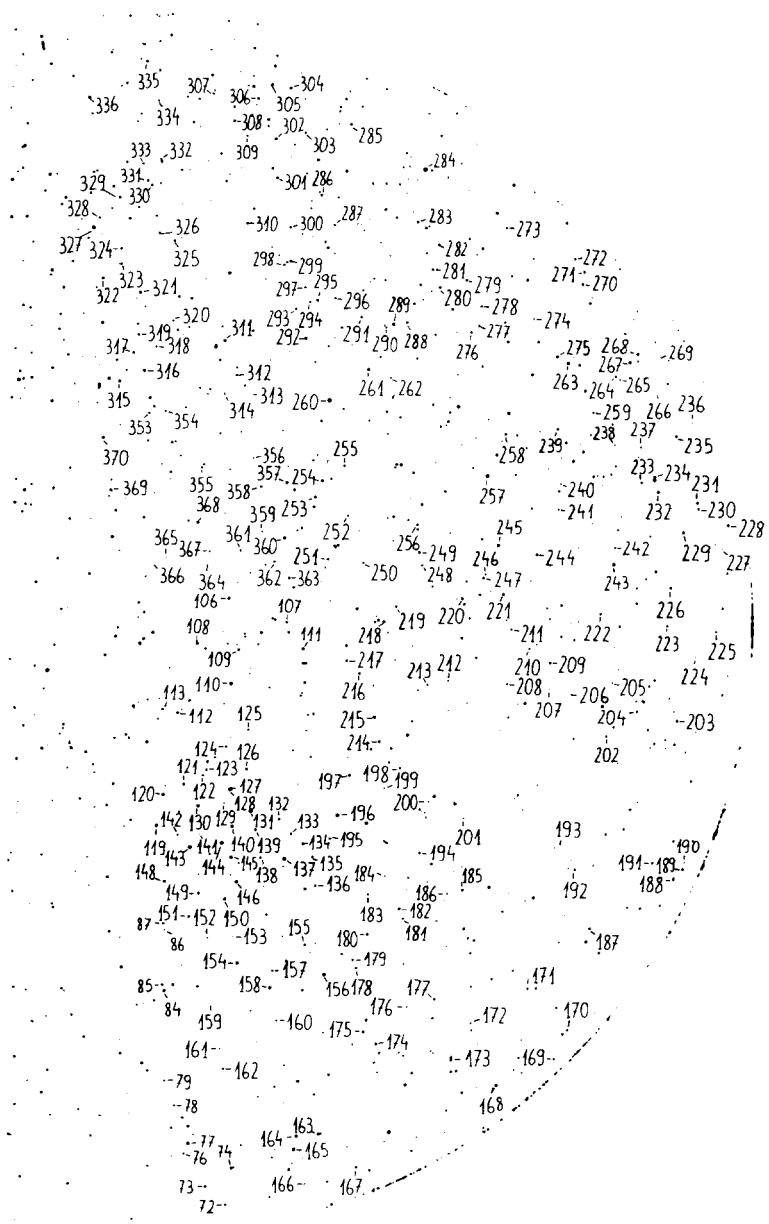

Finding chart of the survey stars

TABLE

Spectra and UBV data of survey stars

No.	Sp.	V	B-V	U-B	remarks
1	A3	8.45	0.42	0.07	BD +4°3481
2	A4	11.56	0.52	0.05	
3	F7	9.00	0.75	0.13	BD +4°3483
4	F4	11.94	0.79	-0.07	
5	A2	12.24	0.47	0.02	
6	F3	11.72	0.81	-0.02	
7	F2	11.62	0.70	0.19	
8	B6	9.92	0.33	-0.25	BD +3°3480
9	A2	11.87	0.65	0.15	
10	A0:	12.45	0.42	-0.10	
11	F5	11.72	0.64	0.14	
12	A8	12.06	0.68	0.09	
13	F7:	11.28	0.99	0.01	
14	A1	9.82	0.47	0.16	BD +3°3485
15	B8	11.45	0.21	-0.22	
16	F2:	12.39	0.64	-0.01	
17	F6	10.08	0.86	0.23	BD +3°3490, blend
18	F2:	11.51	0.92	-0.08	
19	F3:	11.50	0.91	-0.01	
20	B6	6.32	0.22	-0.10	BD +3°3493
21	F5	9.02	0.56	-0.03	BD +3°3492
22	F2	11.54	0.65	-0.15	
23	B9	12.07	0.29	-0.08	
24	A6	10.96	0.50	0.17	
25	F6	11.44	0.75	0.03	
26	F4:	11.96	0.69	-0.23	
27	A9	11.15	0.43	0.09	
28	F5:	11.92	0.67	-0.17	
29	F3	11.71	0.54	-0.16	
30	F3	11.03	0.60	-0.09	
31	A7	10.73	0.43	-0.03	BD +3°3506
32	F6	9.80	0.62	-0.15	BD +3°3504
33	A8	8.24	0.33	-0.07	BD +3°3505
34	F5	11.09	0.78	-0.02	
35	B6	10.68	0.10	-0.55	BD +3°3533, blend
36	F6	10.31	0.78	0.07	BD +4°3532
37	A3	10.41	0.39	-0.05	BD +4°3531
38	F6	11.15	0.65	-0.14	
39	F6	10.78	0.60	-0.26	
40	A5	10.64	0.31	-0.04	BD +4°3521
41	F3	10.83	0.76	-0.07	
42	A2	11.49	0.58	-0.14	
43	F3	7.41	0.44	-0.07	BD +4°3517
44	F3	11.95	0.41	0.04	blend
45	A1	11.67	0.39	-0.02	
46	A3	10.46	0.38	0.08	BD +4°3515
47	F4	11.20	0.68	0.02	
48	A6	10.33	0.34	0.12	BD +4°3516
49	A9	10.60	0.64	0.09	BD +4°3514
50	A4	11.25	0.65	0.04	BD +4°3513
51	F2	11.51	0.76	-0.13	

TABLE

/ Continued /

No.	Sp.	V	B-V	U-B	remarks
52	A1	11.74	0.62	0.07	
53	F5	11.07	0.85	0.10	
54	A9	7.94	0.45	-0.07	BD +4°3506
55	B9	11.51	0.61	0.06	
56	F3	11.47	0.84	0.03	
57	A2:	12.53	0.25	0.19	
58	F7:	11.44	0.88	0.01	
59	F0	11.40	0.71	0.18	
60	F2:	12.64	0.59	-0.08	
61	F7:	11.55	0.96	0.15	
62	F2	10.84	0.75	0.08	
63	F6	10.36	0.80	0.18	BD +4°3492
64	B6	12.29	0.74	-0.04	
65	F7	9.75	0.73	0.25	BD +5°3459
66	F5	10.99	0.71	-0.05	
67	A7	10.16	0.52	0.13	BD +4°3480
68	F4	10.66	0.54	0.14	BD +4°3475
69	A7	9.28	0.53	0.14	BD +4°3477
70	A1	12.33	0.20	0.08	
71	F6	10.44	0.38	0.14	BD +5°3445
72	F7	10.60	0.50	-0.05	
73	F7	9.63	0.48	0.22	BD +5°3446
74	A7	9.48	0.42	0.12	BD +5°3449
75	F6	11.48	0.63	0.18	
76	F2	11.90	0.52	-0.17	
77	B4	8.78	0.23	-0.53	BD +5°3450
78	F5	11.46	0.66	-0.10	
79	A1	11.54	0.54	-0.05	
80	A8	11.60	0.81	-0.12	
81	F0	9.22	0.46	-0.01	BD +5°3457
82	F4	11.44	0.67	0.23	
83	A6	11.77	0.70	0.02	
84+°	B6	8.77	0.07	-0.22	BD +5°3465
85°	A1	10.38	0.29	0.10	
86°	F6	11.32	0.69	0.02	
87	F4	10.74	0.59	0.08	
88	A1:	12.95	0.24	-0.42	
89	F6	11.06	0.74	0.13	
90	A7	11.27	0.51	0.13	
91	F6	9.45	0.72	0.24	BD +4°3502
92	F7:	11.88	0.73	0.05	
93	F7	11.24	0.79	0.17	
94	F2	11.10	0.59	-0.04	
95	F1	7.49	0.47	0.06	BD +5°3505, blend
96	F1	10.51	0.47	-0.08	BD +4°3523, blend
97	A1	10.33	0.27	0.12	BD +4°3524
98	F2	10.61	0.67	-0.07	BD +4°3525
99	B9	10.64	0.24	-0.04	
100	F5	11.61	0.58	-0.21	
101	A6	8.73	0.32	0.01	BD +5°3512
102	A4	10.48	0.56	-0.25	BD +5°3509

TABLE

/ Continued /

No.	Sp.	V	B-V	U-B	remarks
103	F7	10.43	0.38	0.01	
104	A2	10.84	0.34	-0.05	BD +5°3506
105°	A2	10.42	0.35	-0.17	
106	A1	9.91	0.09	0.02	BD +5°3518
107	A2	10.80	0.31	-0.05	
108	A6	9.20	0.42	-0.11	BD +5°3510
109	A1	10.30	0.33	0.01	BD +5°3507
110°	B7	7.66	0.01	-0.71	BD +5°3504
111	F5	9.97	0.42	-0.21	BD +6°3541
112	F2	10.69	0.49	0.08	BD +5°3502
113	F6	11.21	0.64	-0.17	
114	F5	11.72	0.61	0.02	
115	A0	10.38	0.19	0.10	BD +5°3499
116	A0	10.85	0.31	0.10	BD +5°3495
117	A1	10.76	0.55	0.29	BD +5°3492
118	F7:	11.88	0.76	-0.01	
119	F5	7.95	0.47	-0.10	BD +5°3488
120°	B7	9.05	0.06	-0.44	BD +5°3493
121	F6	9.84	0.65	0.10	BD +5°3496
122+	A4	10.93	0.41	0.14	
123	A2	10.96	0.39	0.14	
124	A8	11.76	0.34	0.07	
125	F1	12.11	0.23	-0.10	
126°	A1	9.97	0.14	0.06	BD +5°3497
127°	B9	10.33	0.24	0.16	
128°	B6	8.10	-0.02	-0.44	BD +5°3494
129	F0	11.62	0.47	0.11	
130+°	B7	8.23	0.10	-0.33	BD +5°3491
131°	B3	7.24	0.02	-0.64	BD +5°3490
132	F6	10.95	0.65	0.13	
133°	A7	10.67	0.42	0.23	BD +5°3485
134+°	A5	10.61	0.32	0.25	
135	F5:	11.68	0.61	0.26	
136+°	F5	11.58	0.53	0.00	
137	A0	7.57	0.11	0.07	BD +5°3481
138+°	F2	11.16	0.47	0.05	
139°	A2	10.52	0.28	0.17	BD +5°3486
140+°	B8	8.83	0.23	0.13	BD +5°3487
141	F3	11.67	0.44	0.11	
142	F2:	11.94	0.75	0.20	
143+°	B3	6.88	-0.01	-0.61	BD +5°3483
144°	B5	7.45	0.01	-0.60	BD +5°3484
145°	B4	7.69	0.02	-0.61	BD +5°3482
146°	B3	7.80	0.10	-0.61	BD +5°3478
147°	A1	9.95	0.39	0.08	BD +5°3480
148°	A1	9.18	0.24	0.00	BD +5°3479
149	A0	10.22	0.06	0.06	BD +5°3477
150+°	A1	9.10	0.17	0.03	BD +5°3476
151+°	A3	9.39	0.30	0.21	BD +5°3473
152	F6	11.22	0.52	0.08	
153	F5	11.79	0.41	-0.02	

TABLE

/ Continued /

No.	Sp.	V	B-V	U-B	remarks
154°	B7	8.38	0.07	-0.24	BD +5°3471
155	F5	10.92	0.53	0.22	
156	A6	7.42	0.40	0.15	BD +6°3514
157+o	A8	11.00	0.39	0.06	
158°	B9	7.98	0.06	-0.19	BD +5°3466
159	F7:	11.76	0.54	0.10	
160	F7	11.22	0.45	0.10	
161	F7	11.28	0.60	0.10	
162	A0	10.82	0.12	0.19	BD +5°3456
163	A9	10.22	0.02	0.18	BD +6°3497
164	F7	9.30	0.53	0.09	BD +6°3496
165	A6	7.70	0.36	0.16	BD +6°3494
166	A9	11.84	0.14	-0.08	
167	F5	11.31	0.49	-0.11	
168	F5	9.19	0.53	-0.26	BD +6°3501
169	F6	10.32	0.56	-0.44	BD +7°3444, edge
170	F7	10.81	0.81	0.09	BD +7°3448
171	F3	11.23	0.48	0.08	BD +6°3513
172	F7:	11.80	0.72	-0.07	
173	F5	10.56	0.58	0.13	
174	F6	9.62	0.61	0.05	BD +6°3507
175	A2	10.12	0.17	0.14	BD +6°3508
176	F4:	12.40	0.36	-0.05	
177	A2	11.84	0.16	0.10	
178	F3	11.29	0.57	0.03	
179	A6	11.29	0.49	-0.04	
180	A1	10.72	0.17	0.22	BD +6°3516
181	F6	11.92	0.38	0.07	
182	F2	10.52	0.42	-0.04	BD +6°3518
183	F0	11.80	0.55	0.05	
184	F4:	11.99	0.51	-0.23	
185	A7	10.50	0.40	0.07	BD +6°3521
186	F5:	11.92	0.60	-0.25	
187	F7	10.80	0.61	0.10	
188	A2	10.76	0.44	0.00	BD +7°3459
189	F7	8.87	0.95	0.17	BD +7°3460
190	A1	11.89	0.29	-0.15	
191	F7	11.14	0.56	0.15	
192	F7:	12.38	0.65	0.23	
193	F7:	12.35	0.46	0.03	
194	F2	11.79	0.49	-0.09	
195°	F6	11.39	0.54	-0.04	BD +6°3523
196°	B6	7.88	0.01	-0.77	BD +6°3525
197	F6	10.35	0.63	-0.11	BD +6°3529
198	A1	11.59	0.25	0.14	
199	A0:	12.62	0.17	0.02	
200	A3:	12.88	0.06	0.09	blend
201	F7	11.89	0.60	-0.13	
202	A1	11.45	0.32	0.36	
203	F1	9.98	1.04	0.39	blend
204	F1	11.79	0.42	0.25	

TABLE

/ Continued /

No.	Sp.	V	B-V	U-B	remarks
205	B9:	12.20	0.30	0.03	
206	A0	12.76	0.03	0.03	
207	F3	11.87	0.47	0.00	
208	F5:	11.67	0.43	0.16	
209	A0	10.90	0.23	0.13	BD +7°3472
210	F6	11.31	0.58	0.13	
211	F7	11.40	0.57	0.30	
212	F4:	11.87	0.66	-0.10	
213	F7:	11.73	0.51	-0.10	
214	A6	10.87	0.37	0.03	
215°	A0	9.42	0.10	-0.07	BD +6°3533
216	F0	10.73	0.44	0.02	BD +6°3539
217	F5	11.45	0.54	-0.17	
218	F5	10.04	0.56	-0.14	BD +6°3546
219	F4	11.19	0.52	-0.05	
220	F5	10.23	0.47	0.08	BD +6°3548
221	F3	9.68	0.42	0.24	BD +6°3549
222	F1	11.13	0.37	0.26	
223	F5	11.07	0.55	0.22	
224	F4:	11.61	0.69	0.16	
225	F7	10.48	0.50	0.20	
226	A1	10.04	0.28	0.30	BD +7°3478
227	F5:	11.23	0.56	0.01	
228	F6	8.79	0.83	0.55	BD +7°3485, edge
229	A0	9.62	0.19	0.18	BD +7°3484
230	A2	10.53	0.41	0.08	
231	F6	9.20	0.61	0.33	BD +7°3486
232	F2	8.74	0.47	0.25	BD +7°3487
233	A0	11.20	0.38	0.06	
234	A0	10.27	0.11	0.11	
235	A5	9.87	0.36	0.28	BD +7°3494
236	F6	11.09	0.80	-0.06	
237	F6	11.24	0.59	0.18	blend
238	F2	11.66	0.51	0.00	
239	A6	11.01	0.39	0.10	
240	F4:	12.05	0.51	0.04	
241	F5:	11.79	0.53	0.22	
242	F7:	11.67	0.56	0.14	
243	F6	7.64	0.44	-0.02	BD +7°3481
244	F5	10.11	0.49	0.18	BD +6°3550
245	A0	8.74	0.15	0.13	BD +6°3553
246	F3	11.97	0.54	0.14	
247	F7	11.52	0.55	0.20	
248	F6	11.79	0.50	0.16	
249	F4	10.54	0.50	0.18	BD +6°3551
250	A0	12.18	0.31	0.09	
251	A8	11.63	0.28	0.00	
252	F0	12.04	0.28	-0.27	
253	A3	10.12	0.20	0.10	BD +6°3557
254	A5	10.15	0.40	0.24	BD +6°3559
255	F7	11.37	0.57	0.22	

TABLE

/ Continued /

No.	Sp.	V	B-V	U-B	remarks
256	F3	10.80	0.48	0.17	
257	F5	7.54	0.42	-0.01	BD +6°3560
258	F6	10.71	0.55	0.18	
259	F3	11.58	0.34	0.26	
260	F2	5.70	0.54	-0.10	BD +6°3566
261	A2	9.93	0.26	0.20	BD +6°3568
262	F5:	12.20	0.53	0.05	
263	F7	8.54	0.63	0.07	BD +7°3499
264	F6	11.49	0.71	0.07	
265	F4:	12.02	0.68	0.01	
266	F5:	11.84	0.66	0.19	
267	A4	9.28	0.32	0.20	BD +7°3490
268	A1	9.90	0.21	0.05	BD +7°3502
269	B7:	12.45	0.69	-0.05	
270	A8	10.58	0.56	0.28	BD +7°3504, blend
271	A1	10.14	0.36	0.32	BD +7°3505, edge
272	A5	11.48	0.71	0.11	
273	F7	11.48	0.69	0.15	
274	A1	12.01	0.45	0.23	
275	F0	9.61	0.44	0.28	BD +7°3501
276	F4	11.32	0.59	0.12	
277	A2	11.77	0.22	0.12	
278	A6	11.65	0.43	0.24	
279	F5	10.50	0.64	0.15	
280	A3	10.22	0.40	0.25	BD +6°3573
281	F7	11.12	0.59	0.16	
282	A3	10.94	0.37	0.12	
283	A6	10.98	0.47	0.17	
284	B4	6.19	0.19	-0.36	BD +6°3578
285	F2	11.05	0.57	0.27	BD +6°3580
286	A3	11.47	0.38	0.13	
287	F7:	11.54	0.72	0.24	
288	F5	11.65	0.56	0.20	
289	A3	9.75	0.30	0.17	BD +6°3570
290	F5:	12.55	0.31	0.07	
291	F6	11.03	0.82	0.16	
292	A4	9.56	0.43	0.22	BD +6°3569
293	F7:	11.69	0.71	0.30	blend
294	F4	11.44	0.60	0.08	
295	A0	10.37	0.23	0.10	BD +6°3572
296	F6	11.76	0.57	0.02	
297	F5:	11.65	0.62	0.11	
298	F3	11.32	0.65	-0.03	
299	A1	10.22	0.15	0.00	BD +5°3543
300	F6	11.33	0.73	-0.04	
301	F5	10.29	0.50	-0.08	BD +5°3548
302	A8	10.30	0.56	0.18	BD +5°3550
303	F4	11.68	0.55	0.11	
304	F5	9.12	0.63	0.07	BD +5°3553
305	F3	11.16	0.61	0.18	BD +5°3554
306	F6	10.93	0.71	0.18	

TABLE

/ Continued /

No.	Sp.	V	B-V	U-B	remarks
307	F7:	11.81	0.70	0.13	
308	F0	10.93	0.61	0.12	BD +5°3551
309	F6	11.98	0.62	0.10	
310	A3	11.02	0.32	0.28	
311	A3	9.38	0.38	0.17	BD +5°3535
312	F6	11.62	0.63	0.08	
313	F7:	14.53	-	-	
314	F5	12.12	0.49	-0.01	
315	F6	9.50	0.68	0.08	BD +5°3531
316	B9	9.03	0.23	0.07	BD +5°3533
317	F6	11.26	0.47	0.15	
318	F7:	11.84	0.69	0.03	
319	F6	10.84	0.68	0.11	
320	F6	11.72	0.53	0.13	
321	F4	9.53	0.62	-0.06	BD +5°3540
322	A9	10.95	0.43	0.18	
323	A2	12.07	0.27	0.12	
324	F6	11.11	0.77	0.07	
325	F5	10.68	0.71	0.16	
326	A2	11.91	0.27	0.14	
327	B3	7.47	0.05	-0.69	BD +5°3544
328	F5	11.60	0.48	0.10	
329	A3	10.63	0.39	0.11	BD +5°3545
330	F2	10.82	0.57	0.20	
331	F5	11.44	0.66	0.20	
332	F6	10.42	0.71	0.02	
333	F4	11.61	0.84	0.07	
334	F2	11.94	0.58	0.06	
335	A4:	10.90	0.30	0.48	BD +5°3559, edge
336	F2	8.85	0.58	0.02	BD +5°3552
337	F5	11.31	0.71	-0.03	
338	F7	8.65	0.69	0.04	BD +4°3558
339	F5	11.54	0.47	-0.05	
340	F5	7.55	0.52	-0.25	BD +5°3577
341	A1	9.25	-0.03	-0.62	BD +4°3557
342	A4	10.95	0.38	0.13	
343	F2:	8.87	0.55	0.02	BD +5°3541
344	F2	11.57	0.72	-0.05	
345	F6	11.39	0.54	0.04	BD +4°3547
346	F6	11.63	0.51	-0.01	
347	A1	8.89	0.15	-0.10	BD +5°3537
348	F7	11.51	0.80	-0.02	
349	F3	11.80	0.45	-0.05	
350	A1	10.91	0.49	0.00	
351	B4	7.88	0.03	-0.68	BD +4°3543
352	F6	10.97	0.67	-0.08	
353	F6	11.55	0.69	-0.03	
354	A1	12.35	0.35	0.16	
355	F2	11.38	0.59	0.22	
356	A1:	12.27	0.34	0.01	
357	A4	9.75	0.35	0.38	BD +5°3525, blend

TABLE

/ Continued /

No.	Sp.	V	B-V	U-B	remarks
358	F7	10.95	0.62	0.09	
359	A0:	12.15	0.35	-0.08	
360	F4	8.66	0.48	-0.11	BD +5°3520
361	F6	11.37	0.65	-0.05	
362	F6	11.33	0.51	-0.10	
363	F3	10.97	0.63	-0.13	BD +5°3519
364	F7:	12.12	0.65	-0.11	
365	F4:	12.36	0.53	-0.17	
366	A0	12.98	0.06	-0.10	
367	F7	11.84	0.60	-0.08	
368	A2	9.60	0.18	0.12	BD +5°3523
369	A2	11.65	0.31	0.19	
370	F7	9.98	0.71	0.33	BD +5°3527
371	A9	11.44	0.60	0.00	
372	F7:	12.10	0.67	-0.20	
373	F5:	12.15	0.72	-0.18	
374	A2	9.18	0.20	0.11	BD +4°3539
375	F1	11.63	0.50	-0.25	BD +4°3536
376	F4	11.20	0.57	-0.07	
377	A1	11.67	0.28	0.11	
378	F4	10.94	0.69	-0.20	
379	F7:	12.13	0.56	0.08	
380	B9	8.78	0.22	-0.12	BD +4°3541
381	F6	10.91	0.65	-0.06	
382	F7	10.00	0.59	-0.12	BD +3°3509
383	F3	11.89	0.55	-0.20	
384	F7:	11.55	0.83	-0.13	
385	F7:	12.04	0.59	-0.13	
386	F7:	11.06	0.92	-0.02	
387	F0	10.62	0.58	-0.13	
388	F5	10.84	0.68	-0.09	BD +3°3513
389	F4	9.70	0.63	-0.01	BD +3°3514
390	F7:	11.90	0.96	-0.09	
391	F2:	12.20	0.67	-0.32	
392	A6	11.48	0.30	-0.05	
393	F5	11.56	0.60	-0.12	
394	F5:	11.94	0.75	-0.04	
395	F2:	12.38	0.44	-0.21	
396	A9	8.97	0.37	-0.07	BD +4°3542
397	F7:	12.38	0.65	-0.27	
398	A2:	13.06	0.33	-0.27	
399	F5	12.31	0.54	-0.04	
400	F0	9.00	0.37	-0.07	BD +4°3545
401	A0	12.19	0.24	0.01	
402	F6	11.09	0.74	-0.11	
403	F5	11.85	0.69	-0.19	
404	A4	11.21	0.33	0.03	
405	F0	11.66	0.49	-0.10	
406	F2:	11.85	0.67	-0.01	
407	F4	10.79	0.59	-0.08	
408	A8	11.56	0.49	-0.23	

TABLE

/ Continued /

No.	Sp.	V	B-V	U-B	remarks
409	A0	11.37	0.07	-0.06	blend
410	F6	12.13	0.61	-0.18	
411	F6	11.42	0.60	0.08	
412	A5:	11.18	0.54	0.01	
413	A4	11.07	0.39	0.12	
414	A4	11.28	0.52	0.22	
415	B8	8.11	0.21	-0.12	BD +4°3556
416	F5:	11.65	0.56	0.03	
417	F7:	11.54	0.62	0.14	
418	F5:	11.80	0.58	0.09	
419	A8	9.54	0.40	0.17	BD +4°3551
420	A7	10.64	0.42	0.14	BD +4°3550
421	A1	10.98	0.12	-0.30	
422	F7:	11.69	0.69	-0.04	
423	F6	10.36	0.74	-0.01	BD +4°3559
424	F7:	12.72	1.67	0.61	blend
425	B7:	9.02	0.02	-0.47	BD +4°3560
426	A6	11.61	0.55	-0.05	
427	A3	11.60	0.44	-0.01	

Notes to the table:

A cross and a circle at the right upper side of the running number denotes photoelectrically measured colours and the member of the cluster according to Alcaino, respectively.

A colon beside the spectral types denotes that the star is classified from one plate.

Blend is remarked if the photographic image of the measured star is distorted by a neighbouring star.

Edge is remarked if the star is near the edge of the plate.